



UvA-DARE (Digital Academic Repository)

Advanced endoscopic imaging of esophageal neoplasia; old looks and new visions

Boerwinkel, D.F.

Publication date
2014

[Link to publication](#)

Citation for published version (APA):

Boerwinkel, D. F. (2014). *Advanced endoscopic imaging of esophageal neoplasia; old looks and new visions*. [Thesis, fully internal, Universiteit van Amsterdam].

General rights

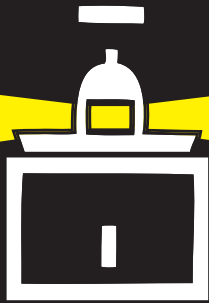
It is not permitted to download or to forward/distribute the text or part of it without the consent of the author(s) and/or copyright holder(s), other than for strictly personal, individual use, unless the work is under an open content license (like Creative Commons).

Disclaimer/Complaints regulations

If you believe that digital publication of certain material infringes any of your rights or (privacy) interests, please let the Library know, stating your reasons. In case of a legitimate complaint, the Library will make the material inaccessible and/or remove it from the website. Please Ask the Library: <https://uba.uva.nl/en/contact>, or a letter to: Library of the University of Amsterdam, Secretariat, Singel 425, 1012 WP Amsterdam, The Netherlands. You will be contacted as soon as possible.

13

DETECTION OF BURIED BARRETT'S GLANDS AFTER RADIOFREQUENCY ABLATION WITH VOLUMETRIC LASER ENDOMICROSCOPY; A HISTOLOGY CORRELATION PILOT STUDY



A Swager; DF Boerwinkel; DM de Bruin; DJ Faber;
AG van Leeuwen; BL Weusten; SL Meijer; JJ Bergman;
WL Curvers

WORK IN PROGRESS

ABSTRACT

BACKGROUND: The prevalence and clinical relevance of Buried Barrett's (BB) epithelium after radiofrequency ablation (RFA) in Barrett's esophagus (BE) is questioned. Recent studies using small optical coherence tomography (OCT) catheters for scanning underneath the neosquamous epithelium demonstrated a high prevalence of tissue structures that might correspond to BB. Histological correlation, however, is lacking. Volumetric Laser Endomicroscopy (VLE) is a novel balloon-based OCT imaging technique that provides a 6-cm long circumferential volumetric scan of the esophageal wall layers to a depth of 3 mm with a resolution comparable to low-power microscopy.

AIM: To evaluate if post-RFA subsquamous structures, detected with VLE, actually correspond to BB and to pursue direct histological correlation of VLE images.

METHODS: In-vivo VLE was performed to detect subsquamous structures suspicious for BB in patients with 100% endoscopic regression of dysplastic Barrett's epithelium after RFA. Areas with suspicious subsquamous VLE structures were marked with electrocoagulation after which in-vivo VLE was repeated to confirm that the correct area was demarcated. These areas were subsequently resected endoscopically, followed by immediate ex-vivo VLE scanning to reconfirm the presence of the subsquamous VLE structures. Extensive histological sectioning was then performed and all histopathology slides were evaluated by an expert BE pathologist (blinded for VLE images).

RESULTS: In 9 patients, 6 areas with suspicious subsquamous structures were seen on in-vivo VLE and resected. Ex-vivo VLE of these 6 ER specimens reconfirmed the presence of these subsquamous structures in 5 ER specimens. Extensive histological sectioning of these areas showed BB in one area. The other subsquamous VLE structures corresponded to dilated (ducts of) (sub)mucosal glands or blood vessels.

CONCLUSION: VLE may potentially detect BB under endoscopically normal appearing neosquamous epithelium. However, most post-RFA subsquamous structures identified by in-vivo VLE did not correspond to BB. Further studies are required to identify VLE features that allow for differentiation of BB from normal subsquamous structures.



INTRODUCTION

In the last decade, endoscopic treatment of early neoplasia in Barrett's esophagus (BE) has become the standard of care. Visible lesions suspicious for intramucosal neoplasia upon endoscopic inspection are removed by endoscopic resection (ER). Residual flat Barrett's epithelium, dysplastic or non-dysplastic, can subsequently be treated with radiofrequency ablation (RFA). RFA uses the emission of radiofrequency energy and ablates the esophageal mucosa until the superficial submucosa (1,2). This leads to eradication of intestinal metaplasia and any residual neoplasia, and recurrence of the normal esophageal squamous mucosa a.k.a. neosquamous epithelium (NSE). RFA has been shown an effective treatment with reported complete eradication of neoplasia of 81-94% and complete eradication of intestinal metaplasia(IM) of 70-77% with a favourable safety profile (3-5).

A potential disadvantage of ablation of BE is the possible occurrence of so called "buried Barrett's" (BB): residual subsquamous Barrett's glands that may remain hidden underneath the NSE. These glands may lead to recurrence of Barrett's epithelium after treatment or may progress to dysplasia or cancer without being detected endoscopically (6,7). The detection of BB with standard endoscopy and biopsy sampling of the NSE is hampered by sampling error due to the scattered spatial distribution of BB and insufficient depth of biopsy sampling (8,9).

Optical frequency domain imaging (OFDI) is an advancement on optical coherence tomography (OCT) that is able to image the superficial wall layers of the esophagus over a large surface area (10,11). Recent OCT studies in patients treated with RFA showed high rates of subsquamous glandular structures (SGS) that might correspond to BB compared to previous biopsy based studies (12,13). These OCT studies are, however, hampered by some important issues. First, in most cases a direct correlation between histology and OCT images was lacking and most structures suspicious for buried Barrett's glands were found within 5 mm proximal from the gastro-esophageal junction (GEJ). Second, the OCT probes utilized only scan one small area at a time. This raises the question whether the structures seen on OCT were "truly" BB, a physiological presence of columnar epithelial outgrowth at the GEJ, or non-Barrett's related glandular structures (e.g. ducts of submucosal glands or bloodvessels).

Volumetric laser endomicroscopy (VLE) (Nvision, NinePoint Medical, Boston, USA) is a new balloon-based OFDI imaging system that generates cross-sectional images over a large circumferential surface area and the full thickness of the esophageal wall.

Major advantage of the VLE system is the possibility of imaging the entire distal esophagus at once at high-resolution and high-acquisition rates, making it a promising tool for investigating the presence of BB in patients treated with RFA.

The aim of this study was to investigate the feasibility of VLE for the detection of subsquamous glandular structures (SGS) underneath the NSE after RFA and directly correlate the VLE findings with histology.

METHODS

Setting

This pilot study was conducted at the department of Gastroenterology and Hepatology of the Academic Medical Center in Amsterdam, a tertiary-care referral centre for patients with Barrett's esophagus and the detection and treatment of early Barrett's neoplasia. This study was approved by the medical ethical committee of the institution (trial nr NTR4056, registered at www.trialregister.nl).

Patients

Patients undergoing endoscopic follow-up after successful endoscopic treatment for BE with high-grade dysplasia (HGD) or early adenocarcinoma (EAC) with RFA with or without prior ER were eligible. Inclusion criteria:

- Complete endoscopic regression of all Barrett's epithelium at all preceding follow-up endoscopies. Complete endoscopic regression was defined as endoscopically normal appearing neo-z-line on inspection with high-resolution white light endoscopy (WLE) and narrow band imaging (NBI) with four biopsies obtained immediately distal to the neo-z-line containing no intestinal metaplasia.
- Circumferential Barrett's extent > 2 cm prior to ablation therapy.
- Written informed consent.

Exclusion criteria:

- Inability to undergo ER and/or obtain biopsies (e.g. due to anticoagulation, coagulation disorders, varices).
- Significant stenosis of the esophagus.
- Erosive esophagitis.

Nvision VLE™ Imaging System

For more comprehensive technical details of the OFDI technique that is used in the Nvision VLE™ Imaging System, we refer to previous publications (14–16). The VLE system consists of a disposable balloon-based catheter and an imaging console. This console which has a display with user interface, is made up of a swept light source, optical receiver and interferometer and a data acquisition computer with control electronics. The console generates near infrared light (bandwidth range 1250 to 1350 nm) and transmits the light into the catheter as a conduit for the laser light source. At its distal end is a polymer, noncompliant balloon (25 mm circumference) with a soft tip. The balloon allows the probe to be placed in the exact centre of the esophageal lumen for in-vivo imaging. Long-segment (6 cm) images can be acquired in 96 seconds over the entire circumference of the distal esophagus till a depth of 3 mm, with an axial-resolution up to 7 µm comparable to low-power microscopy.

With the system it is possible to generate two types of scans. A scout scan is a short scan of 5-10 seconds that enables right positioning of the balloon. A full scan can be acquired when optimal position is attained, using one or more scout scans if necessary. A full scan lasts 96 seconds and acquires data from the full circumference of a 6 cm long trajet of the esophagus.



Endoscopic procedure and VLE scanning

All endoscopic procedures were performed by two expert endoscopists (JB and BW) with extensive experience in examining BE with advanced imaging techniques.

Patients were consciously sedated by intravenous administration of Propofol or Midazolam (2.5-15 mg) supplemented with Fentanyl (0.1-0.2 mg) or Pethidine (25-50 mg) if necessary. The esophagus was first examined in overview with WLE and NBI using a high-definition diagnostic gastroscope (GIF-HQ190, Olympus Inc., Tokyo, Japan) for the detection of residual Barrett's mucosa. After endoscopic examination the gastroscope was switched for a scope with a 3.7 mm working channel that enables introduction of the Nvision VLE catheter.

In order to orientate the endoscopic view with the VLE images three cautery marks were made using the tip of an endoscopic resection snare with pure monopolar coagulation current (forced coagulation effect 2, 40W, ERBE Vio 200D, Erbe Elektromedizin GmbH, Tuebingen, Germany). Cautery marks were placed at approximately 5 mm, 1-2 cm and 3-4 cm above the GEJ at the 12 o'clock position (see figure 1A). Subsequently the VLE catheter was introduced through the working channel of the endoscope and positioned in the distal esophagus including the GEJ. A scout scans were performed to check balloon position. Once the correct position was obtained, a full scan was performed, followed by review of the scan to see if the three orientation markers were visible. If necessary, repositioning of the probe and repeating the scout scans was performed until a good quality full scan containing the orientation markers was obtained.

This full scan was then searched for areas containing SGS (see below). After identification of these areas on the VLE images their position in the esophagus was determined according to the three orientation markers. Subsequently, the probe and balloon were removed from the endoscope. The estimated location of area of interest was then delineated with cautery marks according to the following protocol: two reference cautery marks were placed at the proximal border of the area and two marks at the distal border, which were placed closer together (see figure 1A). In case no SGS were seen, a random area was delineated at the discretion of the endoscopist. After delineation, a second VLE scan of the distal esophagus was performed to confirm the presence of SGS in the delineated area. Based on the second in-vivo scan and the position of the reference markers, ER was performed – including all four reference markers – per standard clinical practice, using the ER-cap method(17). For mucosal lifting saline without adrenaline was used and a hard oblique cap (13.8 mm diameter) was used in order to minimize (post-procedure) complications as bleeding risk. After ER, the resection wound was inspected and photographed and the ER-specimen was retrieved. Finally, four random biopsies were obtained using a standard biopsy forceps under the NSE in the GEJ (<5mm) and in the NSE every 2 cm.

Ex-vivo VLE scanning and ER specimen processing

All ER specimens were pinned on cork containing a grid with 5 mm squares for reference. Based on the position of the cautery marks the ER specimens were orientated in the in-vivo position. In case the in-vivo cautery marks where not sufficient in defining the SGS area location, additional ink markers using a 25-gauge needle were placed on the ER specimen to allow histological correlation of VLE images with areas containing SGS.

After orientation, pinning and additional ex-vivo marking, the resection specimens were placed in a custom designed tubular shaped fixture (figure 1B). The VLE catheter was placed over the ER specimen, the balloon was inflated and VLE scanning was performed. Thereafter the ex-vivo VLE scan was searched for areas containing SGS areas seen on in-vivo VLE. The exact location of the SGS was determined on the ER specimen and indicated on a gridded sketch of the specimen. Finally, the ER-specimen was placed in buffered formalin and fixated for 24 hours minimum.

VLE assessment

Distances and location of the areas containing SGS were recorded during in- and ex-vivo VLE procedure. SGS was defined as the existence of low-scattering round to oval shaped structures of unspecified size, localized in a subepithelial wall layer.

In both in- and ex-vivo VLE scans a manually counted assessment of SGS was performed: number, size (largest and smallest), depth, longitudinal appearance (continuing on a considerable number of subsequent VLE slides), and distance from GEJ (on in-vivo scan) were recorded.

Histological evaluation

After fixation the specimens were sectioned. Both lateral sides of the bottom of the specimen were stained in two different colours to allow correct orientation on histopathology slides. If an area with SGS was present in the specimen, it was sectioned according to the specimen sketch in such a way that the area was included in one paraffin block. The remaining parts of ER specimens without noted SGS were cut every 2-3 mm according to the gridlines, creating histological counterparts as a negative control. After embedding in paraffin blocks, 4 µm histopathology slides were sectioned. Blocks containing SGS areas were extensively sectioned in multiple 4 µm slides, until the entire tissue block was sectioned, with leaps of 3 to 5 slides (~12-20 µm) between every histopathology slide that was processed for analysis. These slides were stained with hematoxylin and eosin (H&E) for histological analysis. All strips were evaluated by an expert gastroenterology

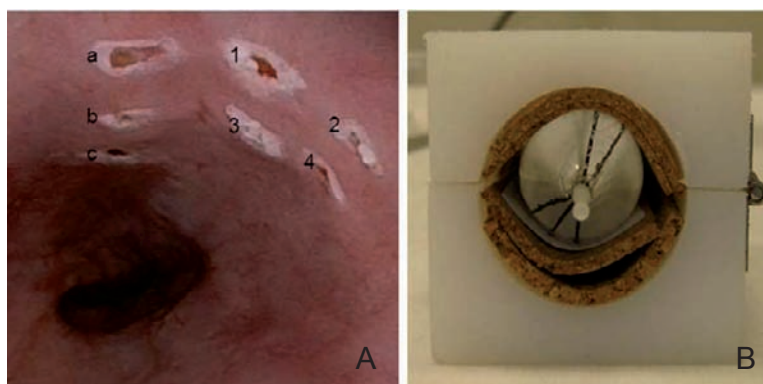


Figure 1. A. In-vivo placement of three orientation cautery marks (a-c) and four reference cautery marks (1-4) for delineation of an SGS area. 1 and 2 represent the 12 o'clock position endoscopically. B. Custom designed tubular shaped fixture for VLE scanning of ER specimen. VLE = volumetric laser endomicroscopy, ER = endoscopic resection.



pathologist (SM) with extensive experience on early Barrett's neoplasia. For correlation with VLE images, selected histopathology slides from areas containing SGS on VLE were digitalized in high resolution tiff images (10x magnified) using the Olympus Slide system (vs 2.5 Tokyo, Japan). The following histological parameters were evaluated: distribution of all layers (mucosa, lamina propria, submucosa, etc.), presence of columnar lined glands under the NSE (number, size and location, presence of intestinal metaplasia and dysplasia) and presence of other subsquamous glandular structures (blood vessels, dilated ducts of submucosal glands, etc.).

RESULTS

Patients

Ten consecutive patients were enrolled undergoing follow-up after RFA. In one patient the VLE-system malfunctioned during the procedure and no ER was performed. Nine patients were included for analysis (mean age 62 years, 8 males). The worst histological diagnosis prior to endoscopic treatment was EAC in 4 patients and HGD in 5. The median circumferential extent of the prior BE segment was 3 cm (IQR 2-5.5) and the median maximum of the BE segment was 6 cm (IQR 4-7.5). Six patients underwent ER and RFA (4 EAC, 2 HGD) and 3 patients only received RFA (all HGD). The median number of RFA treatments (HALO³⁶⁰ and HALO⁹⁰, Bârrx Medical, Sunnyvale, CA) was 3 (IQR 2.5-3). All patients demonstrated complete regression of the Barrett's mucosa and had at least one follow-up endoscopy after endoscopic treatment. The mean time between the last RFA treatment and the study endoscopy was 32 months (range 12-80). Inspection with WLE and NBI at the study endoscopy showed complete endoscopic regression of Barrett's epithelium in all patients. No areas suspicious for residual BE islands or subsquamous abnormalities were identified.

VLE assessment

In total 6 areas with SGS were identified in 6 patients during the first in-vivo VLE scan and were confirmed on the second VLE scan (see flowchart, Figure 2). Mean distance of these SGS from the GEJ was 15 mm (range 0-25 mm). After cautery marking, all areas were endoscopically resected. In 5 of these 6 ER specimens 6 areas containing SGS was identified on ex-vivo VLE (1 specimen contained 2 separate areas). In one ER specimen SGS identified in the two in-vivo VLE scans were not seen on the ex-vivo VLE-scan.

In 3 patients no SGS were identified during in-vivo VLE imaging and according to the protocol 3 random areas were delineated and resected in these patients. In 2 of the 3 patients ex-vivo VLE imaging also showed no SGS. In one patient with no SGS identified on in-vivo VLE, 2 areas with SGS were identified during ex-vivo scanning.

In total 89 different SGS were manually counted in the 6 areas that were identified on in-vivo VLE scans compared to 48 in the 8 areas identified on the ex-vivo scans. The SGS areas appeared as clustered low-scattering round to oval shaped structures that were spread out a few millimetres wide and up to ~600 µm deep. There was no difference in depth location of the SGS in both scans and approximately 30% of the SGS were longitudinal structures.

Histological outcome

All eight areas containing SGS on ex-vivo imaging were enclosed in separate tissue blocks and extensively sectioned for histological evaluation. In one tissue block multiple subsquamous columnar lined glands with intestinal metaplasia (a.k.a Buried Barrett's) were seen on 3 adjacent slides (see figure 3).

In the other SGS areas histology showed blood vessels, dilated ducts of (sub)mucosal glands that likely explained the structures seen on VLE, see figure 4 and 5.

No apparent difference in VLE appearance between SGS that were correlated with BB and other SGS was noted. The area that contained BB, however, had the highest count of SGS in a single area both in-vivo (44 SGS) as ex-vivo (19 SGS) compared to all other areas; with a mean of 14,8 SGS over 6 in-vivo areas and 5,5 SGS over 8 ex-vivo areas.

Negative controls

In addition to extensive sectioning and histological evaluation of areas containing SGS, all ER-specimens were routinely sectioned every 2-3 mm. These routinely sectioned slides (36 in total) acted as negative controls. In none of these slides BB was identified on histological

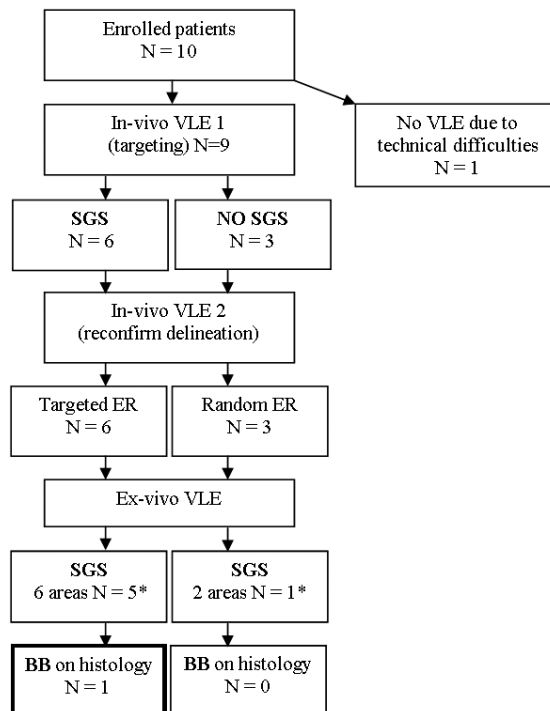


Figure 2. Flowchart showing the number of in-vivo and ex-vivo VLE scans where subsquamous glandular structures (SGS) were visible. VLE = volumetric laser endomicroscopy, ER = endoscopic resection. *1 ER specimen contained 2 separate areas.

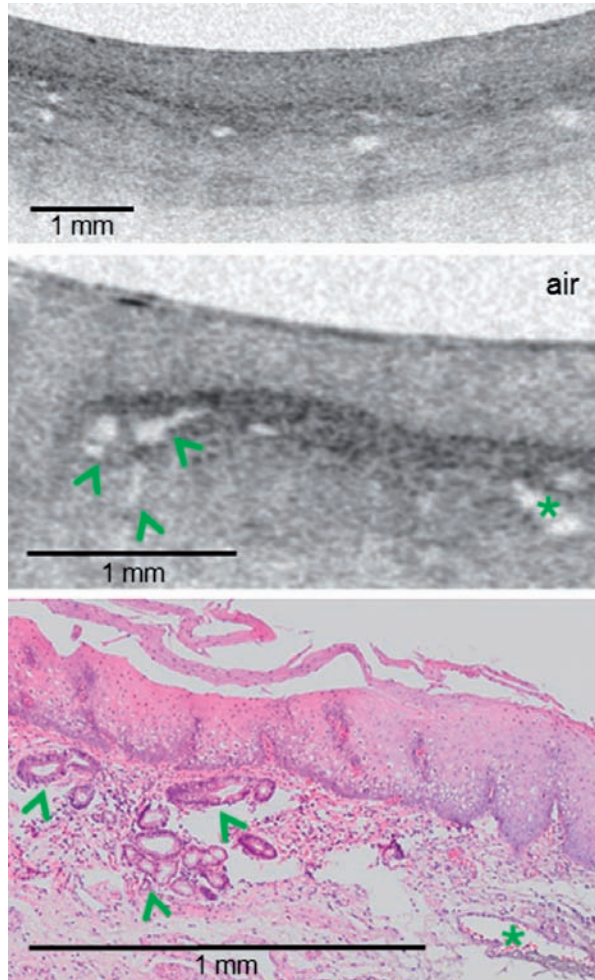


Figure 3. Buried Barrett glands (BB) on in-vivo VLE (A), ex-vivo VLE (B) and corresponding histology (C). Arrowhead indicate BB, asterisk indicates blood vessel. VLE = volumetric laser endomicroscopy.

evaluation. In addition, none of the random biopsies obtained from the NSE or just beneath the GEJ showed either BB or intestinal metaplasia.

DISCUSSION

After treatment with multiple ablation techniques, the phenomenon of BB appearing under the NSE has been described (18–20). Studies on RFA for BE report low percentages of BB prevalence varying between 0 and 5.4% in over 700 patients (3,21,22). Recently, several OCT studies described higher prevalence of SGS, appointed as BB, after RFA on OCT images than previously mentioned studies(12,13). Zhou et al. even reported a presence of BB of 63% (10/16) in patients after RFA treatment (12).

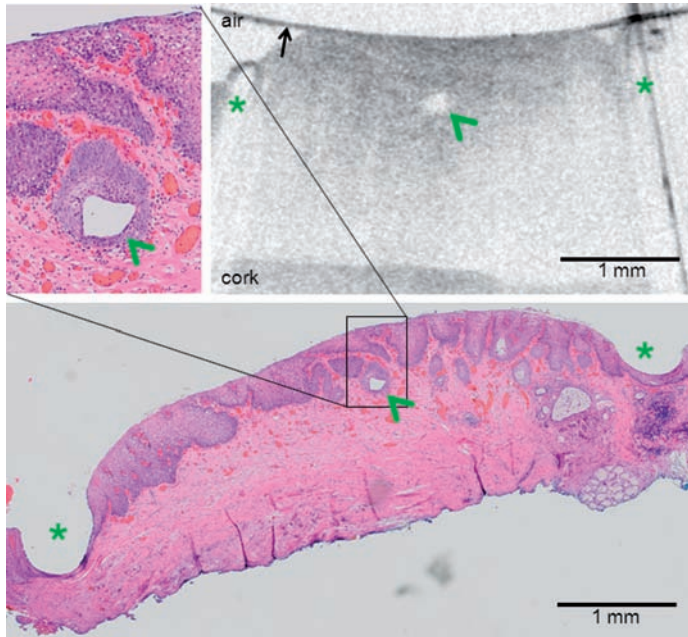


Figure 4. A. Histological image of detailed rendering from C; dilated duct of mucosal gland (arrowhead). B. Corresponding VLE slide of histology slide in C. In both transections 2 pins (asterix) are visible; as long straight structures on VLE and as pin holes on histology. Arrow = VLE balloon. VLE = volumetric laser endomicroscopy.

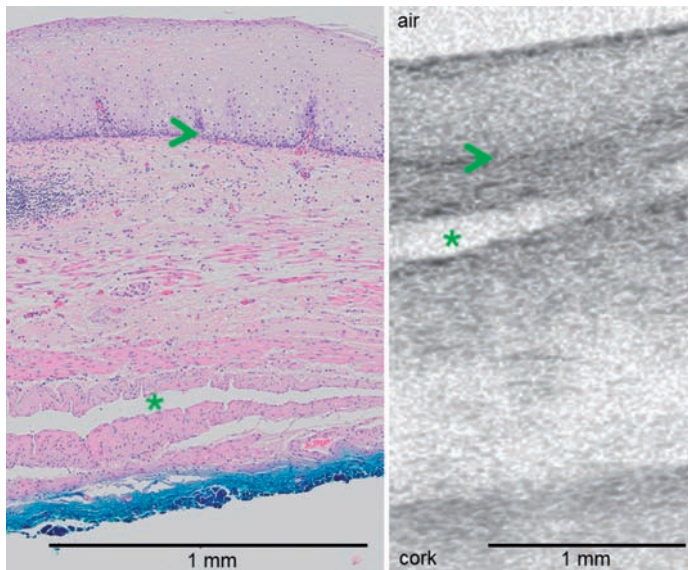


Figure 5. Corresponding histology (A) and VLE slide (B) of blood vessel (asterix). Arrowhead = transition layer from epithelium to lamina propria. VLE = volumetric laser endomicroscopy.



The clinical relevance of BB is debated in literature. In our experience, the prevalence of BB in endoscopically normal NSE is rare (0.1%) and most recurrences of Barrett's epithelium are endoscopically visible (23).

In the current study, we evaluated the feasibility of the OFDI-based VLE system for the detection of BB. VLE provides a 6-cm long circumferential volumetric scan of the esophageal wall layers to a depth of 3 mm with a resolution comparable to low-power microscopy. We used a rigorous protocol, including ER of endoscopically normal appearing NSE to allow for direct histological correlation of VLE findings with histology to overcome the most important limitations of previous studies on the detection of BB (SGS).

First, most studies assessed the presence of BB on random biopsies obtained from the NSE. Random biopsies are, however, inevitably associated with sampling error since only a small area of the NSE is sampled. In addition, biopsy sampling may not reach deep enough in the subepithelial level to identify BB. In literature mixed results are reported on the percentage of biopsies that reach the lamina propria (37-78%) (8,9). VLE scans with a depth of 3 mm, which is sufficient for interrogating the whole submucosa and a circumferential scan of 6 cm in length is obtained thus allowing the evaluation of a large surface area. VLE compares favourably to previous 3D-OCT systems that only scan a small area (8mmx20mmx1.6 mm) (12).

Second, previously mentioned OCT-studies lack direct correlation of the SGS that were detected by OCT and histology. Zhou et al. (12) described 114 subsquamous "Barrett's glands" seen on OCT in 10/16 patients, but only showed histology containing BB from 1 biopsy specimen and 1 ex-vivo ER specimen obtained at the GEJ where BB may be considered a normal physiological finding.

The lack of corresponding histology questions whether all observed structures were indeed BB. In the current study we therefore used a rigorous protocol including in-vivo identification of SGS followed by localization and reconfirmation of the targeted areas in-vivo. Subsequently, ER of the targeted area was performed followed by ex-vivo VLE imaging of the ER specimens to allow for optimal correlation between VLE images and histology.

Targeted ER of areas containing SGS on VLE identified "true BB" in 1 out of 9 patients. In previous studies with random ER of NSE after RFA no BB was seen in a total of 44 patients (5,9) suggesting that targeting areas with SGS on VLE may increase the yield of detecting BB. However, most areas containing SGS on VLE did not show BB upon histological examination. Histological substrates for these SGS were thought to be dilated BE glands, (ducts of) (sub)mucosal glands and blood vessels and were found in the ER specimens. The VLE images of a dilated mucosal gland duct and blood vessel could be correlated to the corresponding histological image (see figure 4 and 5). Cobb et al. described in a OCT-study on esophagectomy specimens that BB can be characterized by a uniform double-band wall appearance (24). After reviewing all areas containing SGS we did not identify any SGS with uniform double-band wall appearance for distinction between BB or other SGS. The axial resolution of VLE (~7 μm) is lower compared to the system used by Cobb et al. (~2.8 μm) and we can therefore not exclude the possibility that at a higher resolution this feature might have been apparent.

The VLE area that contained BB upon histology showed a higher count of SGS in both in- and ex-vivo VLE than other areas, with a number respectively almost 3 and 3,5 times the mean

number of SGS. This characteristic was not noticed on first impression but only after meticulous counting of all glands. A significant number of SGS corresponded with the numerous buried Barrett's glands detected (see figure 3). But also other histological structures such as blood vessels, were seen on the corresponding histology, indicating that part of the SGS on VLE did not correspond with BB. It is questionable whether the number of SGS is a practical and reproducible manner for differentiating BB from other histological structures.

Zhou et al. described that most SGS were identified within the first 5 mm of the neo-z-line. In the GEJ region mucosal overlap is a normal phenomenon where cardia mucosa may undermine the NSE. ER specimens obtained close to the junction may therefore result in a histological artefact of BB (23). We could not confirm these findings in our study. In 8 patients the GEJ was present in the in-vivo VLE scan. After extensive review of the in-vivo scan we only identified a limited number of SGS (< 5) in the GEJ region in 3 patients. These SGS were either not noticed during the initial in-vivo VLE evaluation or were considered less prominent compared to other areas present in the same patient. The area that contained BB was at considerable distance from the GEJ (11 mm). One random ER specimen obtained from the GEJ demonstrated no SGS on in-vivo as well as ex-vivo VLE-imaging and showed no BB on histological evaluation.

Limitations of this study coincide with the complexity of the protocol of performing two in-vivo scans and one ex-vivo scan that were correlated to each other using reference markers. This correlation highly depends on correct orientation from endoscopic view to VLE view. Exactly locating and delineating an endoscopic area with abnormal VLE findings is complex. In two cases inconsistencies between in- and ex-vivo VLE occurred. The first case concerned an in-vivo scan without SGS areas, while 2 areas with SGS were seen on the ex-vivo scan of the (randomly selected) ER specimen. After extensive review of the in-vivo scan, however, no SGS were seen in or around the ER area excluding the possibility of overlooking a SGS area on in-vivo VLE. Another explanation may be that the SGS areas noticed on the ex-vivo scan became visible after ER as a result of tissue manipulation due to the resection, which would hamper ex-vivo VLE examination. Histology of these areas showed indeed manipulated fibrotic tissue and only one dilated duct. In the second case an SGS area was seen during in-vivo VLE while no SGS area was seen on ex-vivo scanning. After reviewing the in-vivo scan we found that the SGS area was probably outside the area that was resected or incorporated in the region that was coagulated during resection. As aforementioned, considering the complexity of this endoscopy protocol these inconsistencies cannot be avoided.

In the current study, we found that ex-vivo VLE showed a different appearance (less SGS, more irregular and less well demarcated) of SGSs compared to in-vivo VLE of the same areas. This discrepancy may be due to changes of the epithelium due to resection, potentially causing structures like blood vessels to collapse. However, it is physiological unlikely that the VLE appearance of BB will change after ER in such a way that BB will not be visible anymore on ex-vivo VLE.

Finally, the period between RFA treatment and study endoscopy was rather prolonged (mean 32 months, range 12-80). Shortening of the treatment-study endoscopy timeframe could possibly increase the yield of detected BB since theoretically presence of BB decreases over time.

In this pilot study we provided reliable histological counterparts of carefully targeted areas containing SGS on VLE. Comprehensive VLE scanning followed by extensive histological



examination of ER specimens of resected SGS areas resulted in the detection of one area with BB in 9 post-RFA patients. Most SGS that were identified on VLE, however, contained non-pathological substrates (e.g. ducts of esophageal submucosal glands or blood vessels). We demonstrated that VLE is able to identify SGS in the esophageal wall, and that some of the SGS correspond to BB, but further studies are required to identify specific VLE-features of BB to optimize detection of BB with VLE.

REFERENCES

- Dunkin BJ, Martinez J, Bejarano PA, Smith CD, Chang K, Livingstone AS, et al. Thin-layer ablation of human esophageal epithelium using a bipolar radiofrequency balloon device. *Surg. Endosc.* [Internet]. 2006;20(1):125–30. Available from: <http://www.ncbi.nlm.nih.gov/pubmed/16333533>
- Ganz RA, Utley DS, Stern RA, Jackson J, Batts KP, Termin P. Complete ablation of esophageal epithelium with a balloon-based bipolar electrode: a phased evaluation in the porcine and in the human esophagus. *Gastrointest. Endosc.* [Internet]. Elsevier; 2004;60(6):1002–10. Available from: <http://www.ncbi.nlm.nih.gov/pubmed/15605025>
- Shaheen N, Sharma P, Overholt BF, Wolfsen HC, Sampliner RE, Wang KK, et al. Radiofrequency Ablation in Barrett's Esophagus with Dysplasia. *N. Engl. J. Med.* 2009;360(22):2277–88.
- Sharma VK, Wang KK, Overholt BF, Lightdale CJ, Fennerty MB, Dean PJ, et al. Balloon-based, circumferential, endoscopic radiofrequency ablation of Barrett's esophagus: 1-year follow-up of 100 patients. *Gastrointest. Endosc.* [Internet]. 2007 Feb [cited 2014 Jan 6];65(2):185–95. Available from: <http://www.ncbi.nlm.nih.gov/pubmed/17258973>
- Phoa KN, Pouw RE, van Vilsteren FGI, Sondermeijer CMT, Ten Kate FJW, Visser M, et al. Remission of Barrett's esophagus with early neoplasia 5 years after radiofrequency ablation with endoscopic resection: a Netherlands cohort study. *Gastroenterology* [Internet]. Elsevier, Inc; 2013 Jul [cited 2013 Nov 7];145(1):96–104. Available from: <http://www.ncbi.nlm.nih.gov/pubmed/23542068>
- Hornick JL, Blount PL, Sanchez CA, Cowan DS, Ayub K, Maley CC, et al. Biologic properties of columnar epithelium underneath reepithelialized squamous mucosa in Barrett's esophagus. *Am. J. Surg. Pathol.* [Internet]. 2005;29(3):372–80. Available from: <http://www.ncbi.nlm.nih.gov/pubmed/15725807>
- Van Laethem JL, Peny MO, Salmon I, Cremer M, Devière J. Intramucosal adenocarcinoma arising under squamous re-epithelialisation of Barrett's oesophagus. *Gut.* 2000;46(4):574–7.
- Shaheen NJ, Peery AF, Overholt BF, Charles J, Chak A, Wang KK, et al. Biopsy depth after radiofrequency ablation of dysplastic Barrett's. *Gastrointest. Endosc.* 2010;72(3):490–6.
- Pouw RE, Gondrie JJ, Rygiel AM, Sondermeijer CM, Ten Kate FJ, Odze RD, et al. Properties of the neosquamous epithelium after radiofrequency ablation of Barrett's esophagus containing neoplasia. [Internet]. *Am. J. Gastroenterol.* Nature Publishing Group; 2009 p. 1366–73. Available from: <http://www.ncbi.nlm.nih.gov/pubmed/19491850>
- Bouma BE, Yun S-H, Vakoc BJ, Suter MJ, Tearney GJ. Fourier-domain optical coherence tomography: recent advances toward clinical utility. *Curr. Opin. Biotechnol.* [Internet]. Elsevier Ltd; 2009;20(1):111–8. Available from: <http://www.pubmedcentral.nih.gov/articlerender.fcgi?artid=2754185&tool=pmcentrez&rendertype=abstract>
- Huang D, Swanson E, Lin C, Schuman J. Optical Coherence Tomography. *Science* (80-.). [Internet]. 1991 [cited 2013 Mar 12];254:1178–81. Available from: <http://onlinelibrary.wiley.com/doi/10.1002/cbdv.200490137/abstract>
- Zhou C, Tsai T-H, Lee H-C, Kirtane T, Figueiredo M, Tao YK, et al. Characterization of buried glands before and after radiofrequency ablation by using 3-dimensional optical coherence tomography (with videos). *Gastrointest. Endosc.* [Internet]. Elsevier Inc.; 2012 Jul [cited 2013 Feb 12];76(1):32–40. Available from: <http://www.pubmedcentral.nih.gov/articlerender.fcgi?artid=3396122&tool=pmcentrez&rendertype=abstract>
- Zhou C, Adler DC, Tsai T-H, Lee H-C, Becker L, Schmitt JM, et al. Endoscopic 3D-OCT Reveals Buried Glands following Radiofrequency Ablation of Barrett's Esophagus. In: Tearney GJ And Wang Td, editor. *Endosc. Microsc. V* [Internet]. 2010. p. 75580L–75580L–6. Available from: <http://link.aip.org/link/PSISDC/v7558/i1/p75580L/s1&Agg=doi>
- Yun SH, Tearney GJ, Vakoc BJ, Shishkov M, Oh WY, Desjardins AE, et al. Comprehensive volumetric optical microscopy in vivo. *Nat. Med.* 2006;12:1429–33.

15. Yun S, Tearney G, De Boer J, Iftimia N, Bouma B. High-speed optical frequency-domain imaging. *Opt. Express* [Internet]. OSA; 2003;11(22):2953–63. Available from: <http://www.pubmedcentral.nih.gov/articlerender.fcgi?artid=3018118&tool=pmcentrez&rendertype=abstract>
16. Vakoc BJ, Shishko M, Yun SH, Oh W, Tearney GJ, Bouma BE. Comprehensive esophageal microscopy by using optical frequency-domain imaging (with video). *Gastrointest. Endosc.* 2007;65(6):898–905.
17. Pouw RE, Van Vilsteren FGI, Peters FP, Herrero LA, Ten Kate FJW, Visser M, et al. Randomized trial on endoscopic resection-cap versus multiband mucosectomy for piecemeal endoscopic resection of early Barrett's neoplasia. *Gastrointest. Endosc.* [Internet]. Elsevier Inc.; 2011;74(1):35–43. Available from: http://www.ncbi.nlm.nih.gov/sites/entrez/?cmd=Retrieve&db=pubmed&dopt=AbstractPlus&query_hl=4&itool=pubmed_DocSum&mynclishare=antonius&list_uids=21704807
18. Mino-Kenudson M, Ban S, Ohana M, Puricelli W, Deshpande V, Shimizu M, et al. Buried dysplasia and early adenocarcinoma arising in Barrett esophagus after porfimer-photodynamic therapy. *Am. J. Surg. Pathol.* [Internet]. 2007;31(3):403–9. Available from: <http://www.ncbi.nlm.nih.gov/pubmed/17325482>
19. Hornick JL, Mino-Kenudson M, Lauwers GY, Liu W, Goyal R, Odze RD. Buried Barrett's epithelium following photodynamic therapy shows reduced crypt proliferation and absence of DNA content abnormalities. *Am. J. Gastroenterol.* [Internet]. 2008;103(1):38–47. Available from: http://www.ncbi.nlm.nih.gov/entrez/query.fcgi?db=pubmed&cmd=Retrieve&dopt=AbstractPlus&list_uids=18076737
20. Gray N, Odze R, Spechler S. Buried Metaplasia After Endoscopic Ablation of Barrett's Esophagus: A Systematic Review. *Am. J. Gastroenterol.* [Internet]. NIH Public Access; 2011;106(11):1899–909. Available from: <http://www.ncbi.nlm.nih.gov/pubmed/18554561>
21. Fleischer DE, Overholt BF, Sharma VK, Reymunde A, Kimmey MB, Chuttani R, et al. Endoscopic radiofrequency ablation for Barrett's esophagus: 5-year outcomes from a prospective multicenter trial. [Internet]. *Endoscopy.* 2010 p. 781–9. Available from: <http://www.thieme-connect.com/ejournals/abstract/endoscopy/doi/10.1055/s-0030-1255779>
22. Lyday WD, Corbett FS, Kuperman DA, Kalvaria I, Mavrelis PG, Shughoury AB, et al. Radiofrequency ablation of Barrett's esophagus: outcomes of 429 patients from a multicenter community practice registry. *Endoscopy* [Internet]. 2010;42(4):272–8. Available from: <http://aithon.ngcsn.net/netacgi/getref2.pl?ref=P-20146164>
23. Pouw RE, Visser M, Odze RD, Sondermeijer CM, Weusten BLAM, Bergman JJ. Pseudo-buried Barrett's post radiofrequency ablation for Barrett's esophagus, with or without prior endoscopic resection. *Endoscopy.* 2013;11–3.
24. Cobb MJ, Hwang JH, Upton MP, Chen Y, Oelschläger BK, Wood DE, et al. Imaging of subsquamous Barrett's epithelium with ultrahigh-resolution optical coherence tomography: a histologic correlation study. *Gastrointest. Endosc.* [Internet]. American Society for Gastrointestinal Endoscopy; 2010 Feb [cited 2013 Feb 12];71(2):223–30. Available from: <http://www.ncbi.nlm.nih.gov/pubmed/19846077>